Available online at www.sciencedirect.com
SCIENCE DIRECT®
ELSEVIER
International Journal of Solids and Structures 43 (2006) 2110–2125
INTERNATIONAL JOURNAL OF SOLIDS and STRUCTURES
www.elsevier.com/locate/ijsolstr

# Selection of prestress for optimal dynamic/control performance of tensegrity structures

Milenko Masic *, Robert E. Skelton

*Department of Mechanical and Aerospace Engineering, University of California, San Diego, La Jolla, 9500 Gilman Drive, CA 92093-0411, United States*

Received 15 December 2004; received in revised form 14 June 2005
Available online 24 August 2005

**Abstract**

This paper concerns prestress optimization of a tensegrity structure for its optimal LQR performance. A linearized dynamic model of the structure is derived in which the force-density variables that parameterize the prestress of the structure appear linearly. A feasible region for these parameters is defined in terms of the extreme directions of the prestress cone. A numerical method for computing this basis for a structure prestress cone is proposed. The problem is solved using a gradient method that provides a monotonic decrease of the objective function inside the feasible region. A numerical example of a cantilevered planar tensegrity beam is shown.


*Keywords:* Tensegrity; Control; Optimization; Prestress

## 1. Introduction

A tensegrity structure is a prestressable, stable, truss-like system involving string elements. No torque can be applied on its elements since the admissible connections between the elements are ball joints and external loads can only act at the joints. Increased interest in tensegrity structures is a result of several favorable properties resulting from the usage of the strings as structural elements. The presence of these controllable elements makes tensegrity structures suitable for applications that require reconfigurability and large shape changes. Structural efficiency is another reason. Similarly to more traditional composite materials, utilization of materials specialized for tensile loads in tensegrity structures yields lightweight

* Corresponding author. Tel.: +1 858 822 6679; fax: +1 858 822 3107.
*E-mail address:* mmasic@mae.ucsd.edu (M. Masic).

0020-7683/$ - see front matter © 2005 Elsevier Ltd. All rights reserved.
doi:10.1016/j.ijsolstr.2005.06.066

designs. This is because these materials usually have superior mechanical properties over materials available for compressive elements.

Although tensegrity structures posses a clear potential, all of their desirable properties are attainable at a certain cost. A reduced size of the domain of feasible configurations because of specific stability (rigidity) issues is one of them. A significant amount of research has been invested in the study of the related form-finding and rigidity problems that can both be characterized as static problems associated with tensegrity structures, e.g. Pellegrino (1992), Connelly and Whiteley (1996), Vasart Motro (1999), Tibert and Pellegrino (2003), Micheletti (2003),Williamson et al. (2003) and Masic et al. (2005a). A method for optimal mass-to-stiffness ratio design of tensegrity structures have been recently proposed in the work of Masic and Skelton (2004) and Masic et al. (2005b). The present state of the tensegrity research is also characterized by the existence of dynamic models derived by Skelton et al. (2001) and Murakami (2001), and control strategies studied by Sultan et al. (2002), Kanchanasaratool and Williamson (2002) and Masic and Skelton (2005).

This paper investigates the optimal distribution of the prestress in a controlled tensegrity structure by jointly designing the structure and its control. Traditionally, the structure and the control designs have been two separate engineering tasks. Designing a structure first and solving its control problem later is not an effective way of achieving a good performance. This is because the structure design usually completely disregards its future control performance measured by the amount of required control energy, yielding structures with severe limitations on the attainable performance. For certain applications, this is not a critical issue, but for some applications, a simultaneous structure and control design is the only way of achieving very restrictive performance requirements. Although the approach of designing a structure and its control jointly has a clear advantage, mathematical tools for solving this problem are of a limited scope because of the non-convex nature of the problem. The available methods for joint structure and control optimization provide at most a convergence to a local minimum. These include results of Skelton et al. (1992), Skelton (1995), Lu and Skelton (2000), Camino et al. (2002, 2003). Alkire (2003) studies numerical issues related to linear matrix inequality (LMI) problems similar to those for joint structure and control design in the above references, and to control problems in general, Boyd et al. (1994). Adeli and Saleh (1998) and Saleh and Adeli (1994) offer more insight into computational challenges of their approach and the approach of related references, e.g. Khot (1998), to joint structure and control design problems.

In this paper, we propose an optimization algorithm which seeks the distribution of prestress variables of a tensegrity structure yielding the optimal combined dynamic and control performance (LQR) of the system for a given nodal configuration, support conditions and load scenario. The solution algorithm iterates on a sequence of LQR problems involving algebraic Riccati equation.

The paper is outlined as follows. In Section 2, a nonlinear model of a tensegrity structure is derived. A linearized model is computed in Section 3, along with the definition of the feasible set of the design parameters. Section 4 defines the problem and the solution algorithm. A numerical example is given Section 5.

## 2. A lumped mass dynamic model of a tensegrity structure

Tensegrity structures can be regarded as a special class of truss structures. Different nonlinear dynamic models of these prestressable structures are available in the literature, e.g. Murakami (2001) and Skelton et al. (2001). Although linear dynamic models of truss structures, and prestressed trusses are well documented, e.g. Hughes (1987) and Murakami (2001), we derive a lumped-mass model here for a few reasons. First, this derivation introduces several useful notions related to tensegrity structures, and it results in a simple and compact representation of the model that clearly display its structure and the structure of the related matrices. This greatly simplifies the subsequent computations of the gradients of performance measures with respect to structural parameters. The entire analysis is performed in global coordinates of an assembled structure. We bypass modelling dynamics of elements in local coordinates and eliminate

the need for the transformation to global coordinates and later assembly which may obscure the algebraic structure of the model.

Let the set $\mathbb{N}$ of $n_{\mathrm{n}}$ nodes of a tensegrity structure be given, and let the node $v_j \in \mathbb{N}$ be located at the position defined by the nodal vector $\mathbf{p}_j \in \mathbb{R}^3$. Denote the set of all nodal vectors $\mathbb{P}$. Let $\mathbb{R}^n_m$ denote the vector space of vectors $\mathbf{x}$ that have the following structure:

$$\mathbf{x} \in \mathbb{R}^n_m \Rightarrow \mathbf{x}^{\mathrm{T}} = \begin{bmatrix} \mathbf{x}_1^{\mathrm{T}} & \mathbf{x}_2^{\mathrm{T}} & \dots & \mathbf{x}_n^{\mathrm{T}} \end{bmatrix}, \quad \mathbf{x}_i \in \mathbb{R}^m, \ \ \mathbb{R}^m = \mathbb{R}^m_1. \tag{1}$$

Then, the set of nodal vectors can be represented with the vector of nodal positions $\mathbf{p} \in \mathbb{R}^{n_{\mathrm{n}}}_3$.

Let the set $\mathbb{E}$ of $n_{\mathrm{e}}$ elements of the structure be given, and let $\mathbb{E}_{\mathrm{s}}$ and $\mathbb{E}_{\mathrm{b}}$ denote its partitions into the sets of $n_{\mathrm{s}}$ strings and $n_{\mathrm{b}}$ bars respectively. The definition of the element $e_i = \{[v_j, v_k], z_i\} \in \mathbb{E}$ of the structure contains the nodes $v_j$ and $v_k$ that it connects, and the scalar identifier, $z_i$, of the type of the element

$$z_i = \begin{cases} 1, & e_i \in \mathbb{E}_{\mathrm{s}}, \\ -1, & e_i \in \mathbb{E}_{\mathrm{b}}. \end{cases} \tag{2}$$

Define element mass vector, $\mathbf{m} \in \mathbb{R}^{n_{\mathrm{e}}}$, by associating its typical element, $m_i \in \mathbb{R}^+$, with every element $e_i$. Assume that the distribution of the mass of the structure is such that it is concentrated at the nodes, so that one half of the mass, $m_i$, of each element is lumped at each of the nodes that it connects. We define the nodal mass vector $\mathbf{m}^{\mathrm{n}} \in \mathbb{R}^{n_{\mathrm{n}}}$ with the entries $m^{\mathrm{n}}_i \in \mathbb{R}^+$ associated with every node $v_i$. Newton's law represents a starting point for deriving a dynamic model of the structure approximated by a system of material points connected with the elements. Let $\mathbf{f}^{\mathrm{n}}(\mathbf{p}, \dot{\mathbf{p}})$, $\mathbf{f}^{\mathrm{e}}(\mathbf{p}, \dot{\mathbf{p}})$ and $\mathbf{f}^{\mathrm{c}}(\mathbf{p}, \dot{\mathbf{p}})$ represent contributions of internal element forces, external forces, and nonworking constraint forces to the total force at each of the nodes, respectively. The dynamics of the system of material points can be defined by the following collection of equations:

$$m^{\mathrm{n}}_i \ddot{\mathbf{p}}_i = \mathbf{f}^{\mathrm{n}}_i(\mathbf{p}, \dot{\mathbf{p}}) + \mathbf{f}^{\mathrm{e}}_i(\mathbf{p}, \dot{\mathbf{p}}) + \mathbf{f}^{\mathrm{c}}_i(\mathbf{p}, \dot{\mathbf{p}}), \quad v_i \in \mathbb{N}. \tag{3}$$

Clearly, both elastic and dumping components of the element forces in $\mathbf{f}^{\mathrm{n}}(\mathbf{p}, \dot{\mathbf{p}})$ are collinear with the elements of the structure. If the element vector $\mathbf{g}_i \in \mathbb{R}^3$ of the element $e_i = \{[v_j, v_k], z_i\}$ is defined as

$$\mathbf{g}_i = \mathbf{p}_j - \mathbf{p}_k, \qquad \|\mathbf{g}_i\|_2 = l_i,$$

then the vector of element vectors $\mathbf{g} \in \mathbb{R}^3_{n_{\mathrm{e}}}$ can be written in the compact form

$$\mathbf{g} = \mathbf{M}(\mathbb{E})\mathbf{p} \tag{4}$$

and the element force vector $\mathbf{f}_{ji} \in \mathbb{R}^3$, that represents the contribution of the internal force of the element $e_i$, to the total force at the node $v_j$, can be expressed as

$$\mathbf{f}_{ji} = c_{ji}(\lambda_i + \lambda^{\mathrm{d}}_i)\mathbf{g}_i, \quad \text{with} \quad f_i = (\lambda_i + \lambda^{\mathrm{d}}_i)\|\mathbf{g}_i\| = (\lambda_i + \lambda^{\mathrm{d}}_i) l_i, \tag{5}$$

where the element elastic, and damping force densities $\lambda_i$, and $\lambda^{\mathrm{d}}_i$, are scalars. Obviously, scalars $c_{ji}$ in (5) that we define as typical elements of the node-element incidence matrix $C(\mathbb{E}) \in \mathbb{R}^{n_{\mathrm{n}} \times n_{\mathrm{e}}}$, have one of the three possible values, $c_{ji} = \pm 1$, or $c_{ji} = 0$. One can verify that the nodal mass vector may be written now as

$$\mathbf{m}^{\mathrm{n}} = 0.5\,\mathrm{abs}(C)\mathbf{m}, \tag{6}$$

where abs denotes the absolute value operator, which in case of a matrix operates on its entries.

Define the linear operator $\tilde{\cdot}$ acting on the vector $\mathbf{x} \in \mathbb{R}^n_m$ as follows:

$$\tilde{\mathbf{x}} := \mathrm{blockdiag}\{\mathbf{x}_1, \dots, \mathbf{x}_i, \dots, \mathbf{x}_n\} \in \mathbb{R}^{mn \times n}, \quad \mathbf{x}_i \in \mathbb{R}^m$$

and the linear operator $\hat{(\cdot)}$ acting on the vector $\mathbf{x} \in \mathbb{R}^n$ by the following Kronecker product:

$$\hat{\mathbf{x}} := \tilde{\mathbf{x}} \otimes I_3 \in \mathbb{R}^{3n \times 3n}. \tag{7}$$

By defining the matrix $\mathbf{C} = C \otimes I_3$, lumping all internal element forces at the nodes can be written in a compact form that defines the total nodal force vector

$$\mathbf{f}^{\mathrm{n}}(\mathbf{p}, \dot{\mathbf{p}}) = \mathbf{C}\tilde{\mathbf{g}}(\mathbf{p})(\boldsymbol{\lambda}(\mathbf{p}) + \boldsymbol{\lambda}^{\mathrm{d}}(\mathbf{p}, \dot{\mathbf{p}})). \tag{8}$$

An equivalent form of this relationship can be obtained using the properties of the related vector operators

$$\mathbf{f}^{\mathrm{n}}(\mathbf{p}, \dot{\mathbf{p}}) = \mathbf{C}(\hat{\boldsymbol{\lambda}}(\mathbf{p}) + \hat{\boldsymbol{\lambda}}^{\mathrm{d}}(\mathbf{p}, \dot{\mathbf{p}}))\mathbf{g}(\mathbf{p}). \tag{9}$$

It is possible to show that the matrices $\mathbf{M}$ and $\mathbf{C}$ satisfy the following relationship, $\mathbf{C}^{\mathrm{T}} = -\hat{\mathbf{z}}\mathbf{M}$. For more details on definitions of these matrices and vectors defined so far consult Masic et al. (2005a).

The relationship between the elastic and damping force-density variables, $\boldsymbol{\lambda} \in \mathbb{R}^{n_e}$ and $\boldsymbol{\lambda}^{\mathrm{d}} \in \mathbb{R}^{n_e}$, and different structural parameters depends on a particular material model. Let cross-sectional areas, Young's modulus, rest-lengths, and viscous damping coefficients of the elements be given in the following vectors: $\mathbf{a}, \mathbf{y}, \mathbf{l}_0, \boldsymbol{\mu} \in \mathbb{R}^{n_e}$. In the case of a linear elastic material, the relationship between the elastic force-density variables, and the structure parameters is given by the Hooke's law

$$\lambda_i(\mathbf{p}, \mathbf{l}_0) = \begin{cases} z_i \dfrac{y_i a_i}{l_i(\mathbf{p}) l_{0_i}} (l_i(\mathbf{p}) - l_{0_i}), \\ 0, \quad \text{if } e_i \in \mathbb{E}_{\mathrm{s}} \text{ and } l_i(\mathbf{p}) \leqslant l_{0_i}. \end{cases} \tag{10}$$

Assume that the elements of the structure are subject to a viscous damping, and that the magnitude of the damping force in the element $e_i$, is proportional to the rate of change of its length, $\dot{l}_i$. We define the damping force-density variables as the magnitudes of the element damping forces per unit length of the corresponding elements, that is

$$\lambda_i^{\mathrm{d}}(\mathbf{p}, \dot{\mathbf{p}}) = \begin{cases} z_i \dfrac{1}{l_i(\mathbf{p})} \mu_i \dot{l}_i(\mathbf{p}, \dot{\mathbf{p}}), \\ 0, \quad \text{if } e_i \in \mathbb{E}_{\mathrm{s}} \text{ and } l_i(\mathbf{p}) \leqslant l_{0_i}. \end{cases} \tag{11}$$

The non-smooth nonlinear relationships in (10) and (11) reflect the fact that the string elements can only transmit a tensional load.

Finally, (3), (8), (10) and (11) define the nonlinear lumped mass model of a tensegrity structure.

## 3. A linearized dynamic model of the structure

A linearized dynamic model of the structure in the neighborhood of an equilibrium configuration is computed in this section. Assume that the structure is stationary in the equilibrium configuration, $\mathbf{p}$, so that $\dot{\mathbf{p}} = 0$. Assume further that all strings are taut and that they remain taut if the structure undergoes a small change of configuration, $\delta\mathbf{p}$. With these assumptions, (10) and (11) can be written in the compact forms

$$\boldsymbol{\lambda}(\mathbf{p}, \mathbf{l}_0) = \tilde{\mathbf{z}}\tilde{\mathbf{l}}^{-1}\tilde{\mathbf{l}}_0^{-1}\tilde{\mathbf{y}}\tilde{\mathbf{a}}(\mathbf{l}(\mathbf{p}) - \mathbf{l}_0), \tag{12}$$

$$\boldsymbol{\lambda}^{\mathrm{d}}(\mathbf{p}, \dot{\mathbf{p}}) = \tilde{\mathbf{z}}\tilde{\mathbf{l}}^{-1}\tilde{\boldsymbol{\mu}}\dot{\mathbf{l}}(\mathbf{p}, \dot{\mathbf{p}}). \tag{13}$$

In the absence of the external and constraint forces, so that $\mathbf{f}^{\mathrm{e}}(\mathbf{p}, \dot{\mathbf{p}}) = 0$, and $\mathbf{f}^{\mathrm{c}}(\mathbf{p}, \dot{\mathbf{p}}) = 0$, the equations in (3) reduce to the following equilibrium conditions:

$$\begin{aligned} &\mathbf{C}\tilde{\mathbf{g}}(\mathbf{p})\boldsymbol{\lambda}(\mathbf{p}, \mathbf{l}_0) = 0, \\ &\lambda_i \geqslant 0, \quad e_i \in \mathbb{E}_{\mathrm{s}}. \end{aligned} \tag{14}$$

In order to linearize the nonlinear dynamic model around this equilibrium, assume that the structure undergoes an infinitesimal nodal displacement $\delta\mathbf{p}$ from the equilibrium configuration $\mathbf{p}$, and that the nodal

velocities change by an infinitesimal amount, $\delta\dot{\mathbf{p}}$. Assume further that element rest-lengths change by an infinitesimal amount from $\mathbf{l}_0$ to $\mathbf{l}_0 + \delta\mathbf{l}_0$, while all other geometric and structural parameters remain unaltered. The resulting variation of the total nodal forces is

$$\delta\mathbf{f}^{\mathrm{n}} = \frac{\partial\mathbf{f}^{\mathrm{n}}}{\partial\mathbf{p}}\,\delta\mathbf{p} + \frac{\partial\mathbf{f}^{\mathrm{n}}}{\partial\dot{\mathbf{p}}}\,\delta\dot{\mathbf{p}} + \frac{\partial\mathbf{f}^{\mathrm{n}}}{\partial\mathbf{l}_0}\,\delta\mathbf{l}_0 \tag{15}$$

and we define the stiffness matrix of the structure as, $\mathscr{K} = -\partial\mathbf{f}^{\mathrm{n}}/\partial\mathbf{p}$, the damping matrix as $\mathscr{D} = -\partial\mathbf{f}^{\mathrm{n}}/\partial\dot{\mathbf{p}}$, and the matrix of sensitivities of nodal forces to rest-length variations as, $\mathscr{B}_{l_0} = \partial\mathbf{f}^{\mathrm{n}}/\partial\mathbf{l}_0$. Using (8), and already established relationships, we have that

$$\delta\mathbf{f}^{\mathrm{n}} = \left(\frac{\partial\mathbf{f}^{\mathrm{n}}}{\partial\mathbf{g}}\,\frac{\partial\mathbf{g}}{\partial\mathbf{p}} + \frac{\partial\mathbf{f}^{\mathrm{n}}}{\partial\boldsymbol{\lambda}}\,\frac{\partial\boldsymbol{\lambda}}{\partial\mathbf{p}} + \frac{\partial\mathbf{f}^{\mathrm{n}}}{\partial\boldsymbol{\lambda}^{\mathrm{d}}}\,\frac{\partial\boldsymbol{\lambda}^{\mathrm{d}}}{\partial\mathbf{p}}\right)\delta\mathbf{p} + \frac{\partial\mathbf{f}^{\mathrm{n}}}{\partial\boldsymbol{\lambda}^{\mathrm{d}}}\,\frac{\partial\boldsymbol{\lambda}^{\mathrm{d}}}{\partial\dot{\mathbf{p}}}\,\delta\dot{\mathbf{p}} + \frac{\partial\mathbf{f}^{\mathrm{n}}}{\partial\boldsymbol{\lambda}}\,\frac{\partial\boldsymbol{\lambda}}{\partial\mathbf{l}_0}\,\delta\mathbf{l}_0. \tag{16}$$

From Eq. (8), we have that

$$\frac{\partial\mathbf{f}^{\mathrm{n}}}{\partial\boldsymbol{\lambda}} = \frac{\partial\mathbf{f}^{\mathrm{n}}}{\partial\boldsymbol{\lambda}^{\mathrm{d}}} = \mathbf{C}\tilde{\mathbf{g}}(\mathbf{p}). \tag{17}$$

Also, from (4), it follows that $\partial\mathbf{g}/\partial\mathbf{p} = \mathbf{M}$ which we use to establish a relationship facilitating computation of the derivatives appearing in (16). We write the element length vector, $\mathbf{l}$, in the equivalent quadratic form

$$\tilde{\mathbf{l}}\mathbf{l} = \tilde{\mathbf{g}}^{\mathrm{T}}\mathbf{g} \tag{18}$$

and, differentiating the left-, and the righthand side of this equation, we have that

$$2\tilde{\mathbf{l}}\frac{\delta\mathbf{l}}{\delta\mathbf{p}} = 2\tilde{\mathbf{g}}^{\mathrm{T}}\frac{\delta\mathbf{g}}{\delta\mathbf{p}} = 2\tilde{\mathbf{g}}^{\mathrm{T}}\mathbf{M} \tag{19}$$

and

$$\frac{\delta\mathbf{l}}{\delta\mathbf{p}} = \tilde{\mathbf{l}}^{-1}\tilde{\mathbf{g}}^{\mathrm{T}}\frac{\delta\mathbf{g}}{\delta\mathbf{p}} = \tilde{\mathbf{l}}^{-1}\tilde{\mathbf{g}}^{\mathrm{T}}\mathbf{M}. \tag{20}$$

The rate of changing element lengths $\dot{\mathbf{l}}$ can now be computed as

$$\dot{\mathbf{l}} = \frac{\delta\mathbf{l}}{\delta\mathbf{p}}\,\frac{\delta\mathbf{p}}{\delta t} = \frac{\delta\mathbf{l}}{\delta\mathbf{p}}\,\dot{\mathbf{p}} = \tilde{\mathbf{l}}^{-1}\tilde{\mathbf{g}}^{\mathrm{T}}\mathbf{M}\dot{\mathbf{p}}, \tag{21}$$

yielding,

$$\frac{\partial\dot{\mathbf{l}}}{\partial\dot{\mathbf{p}}} = \tilde{\mathbf{l}}^{-1}\tilde{\mathbf{g}}^{\mathrm{T}}\mathbf{M}. \tag{22}$$

From (21) it is obvious that in the stationary equilibrium of interest we have that $\dot{\mathbf{l}}|_{\dot{\mathbf{p}}=0} = 0$, and, consequently, from the equation in (13) that

$$\boldsymbol{\lambda}^{\mathrm{d}}|_{\dot{\mathbf{p}}=0} = 0, \qquad \left.\frac{\partial\boldsymbol{\lambda}^{\mathrm{d}}}{\partial\mathbf{p}}\right|_{\dot{\mathbf{p}}=0} = 0. \tag{23}$$

The relationship in (9) gives that $\partial\mathbf{f}^{\mathrm{n}}/\partial\mathbf{g} = \mathbf{C}(\hat{\boldsymbol{\lambda}} + \boldsymbol{\lambda}^{\mathrm{d}})$ which in the stationary equilibrium of interest, using (23), reduces to $\partial\mathbf{f}^{\mathrm{n}}/\partial\mathbf{g} = \mathbf{C}\hat{\boldsymbol{\lambda}}$. The derivation of the stiffness matrix is now completed by computing $\partial\boldsymbol{\lambda}/\partial\mathbf{p}$ from (12), and its final form is

$$\mathscr{K}(\boldsymbol{\lambda}, \mathbf{p}, \mathbf{y}, \mathbf{a}) = \mathbf{C}\tilde{\mathbf{g}}\tilde{\mathbf{y}}\tilde{\mathbf{a}}\tilde{\mathbf{l}}^{-3}\tilde{\mathbf{g}}^{\mathrm{T}}\mathbf{C}^{\mathrm{T}} - \mathbf{C}\hat{\boldsymbol{\lambda}}\mathbf{M}. \tag{24}$$

For more detailed derivation of the stiffness matrix consult Masic et al. (2005a).

The derivations of the damping matrix, and matrix $\mathscr{B}_{l_0} = \partial \mathbf{f}^{\mathrm{n}}/\partial \mathbf{l}_0$ involve computing $\partial \boldsymbol{\lambda}^{\mathrm{d}}/\partial \dot{\mathbf{p}}$ and $\partial \boldsymbol{\lambda}/\partial \mathbf{l}_0$ respectively. The equation in (13), using (22) yields

$$\frac{\partial \boldsymbol{\lambda}^{\mathrm{d}}}{\partial \dot{\mathbf{p}}} = \tilde{\mathbf{z}}\tilde{\boldsymbol{\mu}}\tilde{\mathbf{l}}^{-1}\frac{\partial \dot{\mathbf{l}}}{\partial \dot{\mathbf{p}}} = \tilde{\mathbf{z}}\tilde{\boldsymbol{\mu}}\tilde{\mathbf{l}}^{-1}\tilde{\mathbf{l}}^{-1}\tilde{\mathbf{g}}^{\mathrm{T}}\mathbf{M} = -\tilde{\boldsymbol{\mu}}\tilde{\mathbf{l}}^{-2}\tilde{\mathbf{g}}^{\mathrm{T}}\mathbf{C}^{\mathrm{T}}, \tag{25}$$

so that the damping matrix $\mathscr{D}$ can finally be written as

$$\mathscr{D} = \mathbf{C}\tilde{\mathbf{g}}\tilde{\mathbf{l}}^{-2}\tilde{\boldsymbol{\mu}}\tilde{\mathbf{g}}^{\mathrm{T}}\mathbf{C}^{\mathrm{T}}. \tag{26}$$

Similarly, (12) gives that

$$\frac{\partial \boldsymbol{\lambda}}{\partial \mathbf{l}_0} = -\tilde{\mathbf{z}}\tilde{\mathbf{y}}\tilde{\mathbf{a}}\tilde{\mathbf{l}}_0^{-2}, \tag{27}$$

so that finally,

$$\mathscr{B}_{l_0} = -\mathbf{C}\tilde{\mathbf{g}}\tilde{\mathbf{z}}\tilde{\mathbf{y}}\tilde{\mathbf{a}}\tilde{\mathbf{l}}_0^{-2}. \tag{28}$$

Assume that variations of the variables are small so that the finite variation, $\Delta \mathbf{f}^{\mathrm{n}}$, of the total nodal force can be approximated with the first order approximation

$$\Delta \mathbf{f}^{\mathrm{n}} = \sum_i \frac{\partial \mathbf{f}^{\mathrm{n}}}{\partial \mathbf{x}_i}\Delta \mathbf{x}_i, \qquad \mathbf{x}_i = \{\mathbf{p}, \dot{\mathbf{p}}, \mathbf{l}_0\}. \tag{29}$$

We further assume that the external forces that are applied to the structure are independent from a current configuration of the structure, that is $\partial \mathbf{f}^{\mathrm{e}}/\partial \mathbf{p} = 0$, and $\partial \mathbf{f}^{\mathrm{e}}/\partial \dot{\mathbf{p}} = 0$, and we use the following notation, $\mathbf{f}^{\mathrm{e}} = \mathbf{w}(t)$.

Finally, for an unconstrained equilibrium tensegrity structure with $\mathbf{f}^{\mathrm{c}} = 0$, the linearized dynamic model, can be written as

$$\mathscr{M}\ddot{\mathbf{u}} + \mathscr{D}\dot{\mathbf{u}} + \mathscr{K}(\boldsymbol{\lambda}, \mathbf{p}, \mathbf{y}, \mathbf{a})\mathbf{u} = \mathscr{B}_{l_0}\Delta \mathbf{l}_0 + \mathbf{w}, \tag{30}$$

$$\mathscr{K}(\boldsymbol{\lambda}, \mathbf{p}, \mathbf{y}, \mathbf{a}) = \mathbf{C}\tilde{\mathbf{g}}\tilde{\mathbf{y}}\tilde{\mathbf{a}}\tilde{\mathbf{l}}^{-3}\tilde{\mathbf{g}}^{\mathrm{T}}\mathbf{C}^{\mathrm{T}} - \mathbf{C}\hat{\boldsymbol{\lambda}}\mathbf{M}, \tag{31}$$

$$\mathscr{D} = \mathbf{C}\tilde{\mathbf{g}}\tilde{\mathbf{l}}^{-2}\tilde{\boldsymbol{\mu}}\tilde{\mathbf{g}}^{\mathrm{T}}\mathbf{C}^{\mathrm{T}}, \tag{32}$$

$$\mathscr{M} = \hat{\mathbf{m}}^{\mathrm{n}}, \qquad \mathbf{m}^{\mathrm{n}} = 0.5\,\mathrm{abs}(C)\mathbf{m}, \tag{33}$$

$$\mathscr{B}_{l_0} = -\mathbf{C}\tilde{\mathbf{g}}\tilde{\mathbf{z}}\tilde{\mathbf{y}}\tilde{\mathbf{a}}\tilde{\mathbf{l}}_0^{-2}, \tag{34}$$

where $\mathbf{u}$, and $\Delta \mathbf{l}_0$ denote the finite variations of the variables $\mathbf{p}$, $\mathbf{l}_0$ respectively.

The initial assumptions on the distribution of mass of the structure resulted in a diagonal form of the mass matrix. If needed, this model can be modified by adopting a different lumped or consistent mass matrix approximations available in the literature.

### 3.1. Treatment of boundary conditions

The only constraint on structure displacements $\mathbf{u}$ that will be considered here is the consequence of attaching the nodes of the structure to fixed linear supports. In that case, the admissible nodal displacements must satisfy the following linear constraint:

$$C_u\mathbf{u} = 0 \tag{35}$$

and consequently,

$$C_u\dot{\mathbf{u}} = 0, \qquad C_u\ddot{\mathbf{u}} = 0, \tag{36}$$

where the structure of the constraint matrix $C_u \in \mathbb{R}^{n_c \times 3n_n}$ depends on particular support conditions. It can be shown that the constraint forces, $\mathbf{f}^c(\mathbf{u})$, are the vectors in the left range space of the matrix $C_u$ in any configuration $\mathbf{u}$. Hence, $\mathbf{f}^c(\mathbf{u})$ can be expressed as

$$\mathbf{f}^c(\mathbf{u}) = C_u^T \boldsymbol{\lambda}^c(\mathbf{u}) \tag{37}$$

for some choice of the Lagrange multipliers $\boldsymbol{\lambda}^c \in \mathbb{R}^{n_c}$. Assume that only $n_c$ independent boundary conditions are defined so that matrix $C_u$ has a full row rank. Let the singular value decomposition of the matrix $C_u$ be given as

$$C_u = U\Sigma V^T = U[\,\Sigma_1 \quad 0\,]\begin{bmatrix} V_1^T \\ V_2^T \end{bmatrix} = U\Sigma_1 V_1^T, \qquad C_u^T = V_1\Sigma_1 U^T,$$
$$UU^T = U^T U = I, \qquad VV^T = V^T V = I.$$

The relationships in (35) and (36) imply that the admissible nodal displacements and their derivatives must lie in the null space of the matrix $C_u$, so that

$$\mathbf{u} = V_2\underline{\mathbf{u}}, \quad \dot{\mathbf{u}} = V_2\dot{\underline{\mathbf{u}}}, \quad \ddot{\mathbf{u}} = V_2\ddot{\underline{\mathbf{u}}}. \tag{38}$$

Adding the additional term to the linearized dynamic model (30) to account for the presence of the constraint forces given in (37), gives

$$\mathscr{M}\ddot{\mathbf{u}} + \mathscr{D}\dot{\mathbf{u}} + \mathscr{K}(\boldsymbol{\lambda}, \mathbf{p}, \mathbf{y}, \mathbf{a})\mathbf{u} = \mathscr{B}_{l_0}\Delta\mathbf{l}_0 + \mathbf{w} + C_u^T\boldsymbol{\lambda}^c(\mathbf{u}). \tag{39}$$

Multiplication of both sides of (39) from the left with the orthonormal full rank matrix $V^T$, and applying the change of variables in (38) yields

$$\begin{bmatrix} V_1^T \\ V_2^T \end{bmatrix}(\mathscr{M}V_2\ddot{\underline{\mathbf{u}}} + \mathscr{D}V_2\dot{\underline{\mathbf{u}}} + \mathscr{K}(\boldsymbol{\lambda}, \mathbf{p}, \mathbf{y}, \mathbf{a})V_2\underline{\mathbf{u}}) = \begin{bmatrix} V_1^T \\ V_2^T \end{bmatrix}\mathscr{B}_{l_0}\Delta\mathbf{l}_0 + \begin{bmatrix} V_1^T \\ V_2^T \end{bmatrix}\mathbf{w} + \begin{bmatrix} \Sigma_1 U^T \\ 0 \end{bmatrix}\boldsymbol{\lambda}^c(\mathbf{p}). \tag{40}$$

It is clear from (40), that the solution of the problem can be split into two parts. Lagrange multipliers $\boldsymbol{\lambda}^c$ do not appear as the variable in the first set of equations, so that

$$V_2^T\mathscr{M}V_2\ddot{\underline{\mathbf{u}}} + V_2^T\mathscr{D}V_2\dot{\underline{\mathbf{u}}} + V_2^T\mathscr{K}(\boldsymbol{\lambda}, \mathbf{p}, \mathbf{y}, \mathbf{a})V_2\underline{\mathbf{u}} = V_2^T\mathscr{B}_{l_0}\Delta\mathbf{l}_0 + V_2^T\mathbf{w}, \tag{41}$$

while the second set of equations provides the solution for the Lagrange multipliers, and the constraint forces. The minimal representation of the dynamic model is given in terms of the constrained mass, damping and stiffness matrices,

$$\underline{\mathscr{M}}\ddot{\underline{\mathbf{u}}} + \underline{\mathscr{D}}\dot{\underline{\mathbf{u}}} + \underline{\mathscr{K}}(\boldsymbol{\lambda}, \mathbf{p}, \mathbf{y}, \mathbf{a})\underline{\mathbf{u}} = V_2^T\mathscr{B}_{l_0}\Delta\mathbf{l}_0 + V_2^T\mathbf{w}. \tag{42}$$

### 3.2. State space model of the system

We identify nodal displacements $\underline{\mathbf{u}}$ and nodal velocities $\dot{\underline{\mathbf{u}}}$ as the state variables of the system, and $\mathbf{w}$ as exogenous inputs. Control inputs denoted by $\Delta\boldsymbol{\lambda}$ are defined as follows:

$$\Delta\boldsymbol{\lambda} = \frac{\partial\boldsymbol{\lambda}}{\partial\mathbf{l}_0}\Delta\mathbf{l}_0 \tag{43}$$

and they are dimensionally equivalent to variations of elastic element force-densities. Observe that for a given value of the control variable $\Delta\boldsymbol{\lambda}$ the necessary changes of element rest-lengths to produce these variations of scaled element forces can be recovered as $\Delta\mathbf{l}_0 = (\partial\boldsymbol{\lambda}/\partial\mathbf{l}_0)^{-1}\Delta\boldsymbol{\lambda}$ since $\partial\boldsymbol{\lambda}/\partial\mathbf{l}_0$, given in (27), is an invertible static linear mapping.

A parameterized model of the linearized dynamics of the structure may be put in the following state space form:

$$\begin{aligned}
&\dot{\mathbf{x}} = A(\boldsymbol{\lambda})\mathbf{x} + B\Delta\boldsymbol{\lambda} + B_w\mathbf{w},\\
&A = \begin{bmatrix} 0 & I \\ -\underline{\mathscr{M}}^{-1}\underline{\mathscr{K}}(\boldsymbol{\lambda},\mathbf{p},\mathbf{y},\mathbf{a}) & -\underline{\mathscr{M}}^{-1}\underline{\mathscr{D}} \end{bmatrix},\\
&B = \begin{bmatrix} 0 \\ \underline{\mathscr{M}}^{-1}V_2^{\mathrm{T}}\mathbf{C}\tilde{\mathbf{g}} \end{bmatrix}, \qquad B_w = \begin{bmatrix} 0 \\ \underline{\mathscr{M}}^{-1}V_2^{\mathrm{T}} \end{bmatrix}.
\end{aligned} \tag{44}$$

*3.2.1. Identifying the structure design freedom*

It is important to emphasize the fundamental difference between the prestress parameters $\boldsymbol{\lambda}$ and the control variables $\Delta\boldsymbol{\lambda}$. Recall that the prestress parameters, $\boldsymbol{\lambda}$, of the model in (44), represent equilibrium force densities, and any freedom in the model must comply with this constraint. On the other hand, control variables in $\Delta\boldsymbol{\lambda}$ are completely independent from each other and from the equilibrium prestress $\boldsymbol{\lambda}$. Variations of these control variables that can be generated by modifying element rest-lengths, as shown here, induce additional element forces that are in general non-equilibrium forces for the overall structure.

Consider an equilibrium tensegrity structure that in the equilibrium configuration $\mathbf{p}$ has a multidimensional prestress cone with a non-unique basis $\Lambda(\mathbf{p})$, defined in Masic et al. (2005a). The prestress cone of a tensegrity structure represents an intersection of two convex sets, $\boldsymbol{\lambda} = \mathrm{Null}(\mathbf{C}\tilde{\mathbf{g}}(\mathbf{p}))$, and the positive cone characterized by $\lambda_i \geqslant 0$, $e_i \in \mathbb{E}_s$. Hence, feasible force-densities for a given configuration of a tensegrity structure belong to a polyhedral convex cone. In this study, we use a particular basis, denoted $\Lambda^E(\mathbf{p})$, for the polyhedral prestress cone of the structure. This basis is particular in that its columns represent the extreme directions of the polyhedral prestress cone, so that every feasible force-density vector, $\boldsymbol{\lambda} \in \Lambda^E(\mathbf{p})$, can be written as $\boldsymbol{\lambda} = \Lambda^E(\mathbf{p})\underline{\underline{\lambda}}$, for some choice of $\underline{\underline{\lambda}}$ with $\underline{\underline{\lambda}}_i \geqslant 0$. The basis for the prestress cone with this property can be computed applying an algorithm that is derived from an implementation of the simplex method for linear programming. This algorithm seeks and identifies all vertices of the linear constraint $Nx \geqslant 0$. Fig. 2 depicts an application of the algorithm on identifying the extreme directions of the prestress cone of the structure of Fig. 1 that has three prestress modes.

The preceding geometric analysis of the set of feasible prestresses of tensegrity structures assumes that no material or cross-sectional properties are associated with its elements. If such properties are predefined, one must additionally constrain the prestress parameters $\boldsymbol{\lambda}$ to ensure that the actual elements of the structure can be built after defining its prestress. If the cross-sectional area of the elements, denoted $\mathbf{a}$, is given, and the material of the structure is fixed, by fixing its Young's modulus $\mathbf{y}$, this constraint must guarantee that the resulting element rest-lengths are feasible, that is $l_{0_i} > 0$. Hence, from (12), force-density variables must satisfy

$$\lambda_i l_i < y_i a_i, \quad e_i \in \mathbb{E}_b. \tag{45}$$

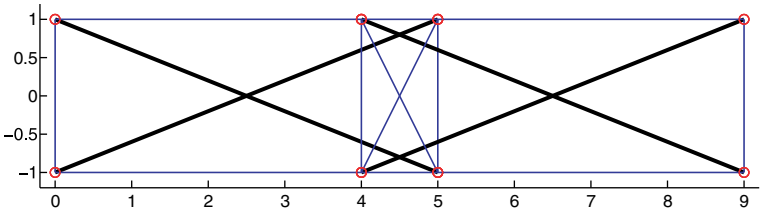


Fig. 1. Tensegrity structure with three prestress modes.

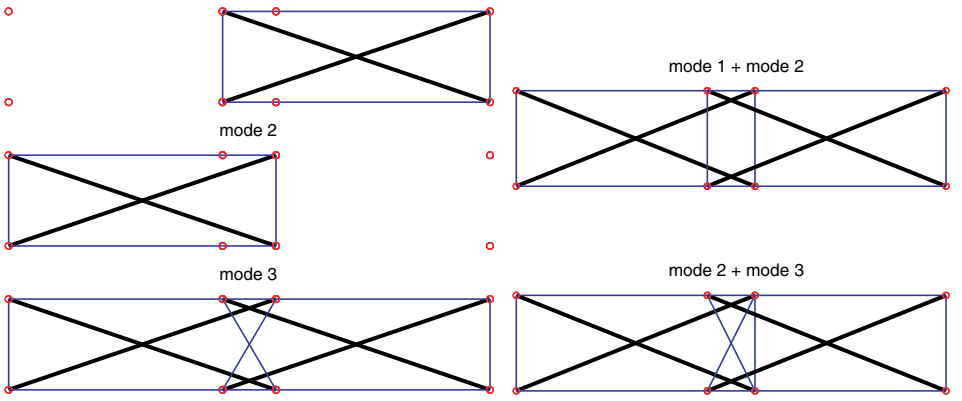


Fig. 2. Left: Extreme directions of the prestress cone of the structure in Fig. 1; Right: Combinations of the prestress modes of the structure; Only elements with nonzero prestress are shown.

Imposing a similar but a more restrictive constraint,

$$\lambda_i < \epsilon_i \frac{y_i a_i}{l_i}, \quad \text{for some } 0 < \epsilon_i < 1, \tag{46}$$

on all elements of the structure ensures that the prestress of the elements does not exceed their yield stress, and constrains the structure from this mode of failure.

## 4. Selection of prestress for optimal LQR performance

### 4.1. Formulation of the problem

Let all parameters defining the model (44) of the structure in Fig. 1 be defined, except its feasible prestress $\underline{\underline{\boldsymbol{\lambda}}}$. We seek the distribution of the prestress, and the state feedback control law $\Delta\boldsymbol{\lambda}(t) = G\mathbf{x}(t)$ of the structure that is subjected to independent zero mean stochastic excitations $\mathbf{w}(t)$, with variance $W$, so that the performance index

$$J(\mathbf{x}, \Delta\boldsymbol{\lambda}) = \lim_{t\to\infty} E\{\mathbf{x}^{\mathrm{T}}(t)Q\mathbf{x}(t) + \Delta\boldsymbol{\lambda}(t)^{\mathrm{T}}R\Delta\boldsymbol{\lambda}(t)\} \tag{47}$$

is minimized. $E\{\cdot\}$ denotes the expectation operator, and positive definite matrix $R \succ 0$ and positive semi-definite matrix $Q \succeq 0$, are given control and output variance penalty matrices. Kwakernaak and Sivan (1972), Skelton (1988) and Zhou and Doyle (1998) offer more details on the LQR problem, including the conditions for the existence of this closed-loop performance index for the system (44).

Assuming that the existence conditions are satisfied, and using properties of the matrix trace operator $\mathrm{Tr}[\cdot]$, it is possible to show that the performance index in (47) has an equivalent algebraic form

$$\begin{aligned} J(\mathbf{x}, \Delta\boldsymbol{\lambda}) = J(\mathbf{x}, G\mathbf{x}) &= \lim_{t\to\infty} E\{\mathrm{Tr}[\mathbf{x}^{\mathrm{T}}(t)(Q + G^{\mathrm{T}}RG)\mathbf{x}(t)]\} = \lim_{t\to\infty} E\{\mathrm{Tr}[(Q + G^{\mathrm{T}}RG)\mathbf{x}(t)\mathbf{x}^{\mathrm{T}}(t)]\} \\ &= \mathrm{Tr}[(Q + G^{\mathrm{T}}RG) \lim_{t\to\infty} E\{\mathbf{x}(t)\mathbf{x}^{\mathrm{T}}(t)\}] = \mathrm{Tr}[(Q + G^{\mathrm{T}}RG)X], \end{aligned} \tag{48}$$

where $X = \lim_{t\to\infty} E\{\mathbf{x}(t)\mathbf{x}^{\mathrm{T}}(t)\}$ can be computed from the following Lyapunov equation:

$$(A + BG)X + X(A + BG)^{\mathrm{T}} + B_w W B_w^{\mathrm{T}} = 0, \quad X \succ 0. \tag{49}$$

Using the relationship between prestress and the structure dynamics that are already established in (44), and the definition of the feasible set of the prestress, a modified formulation of the LQR problem accommodating a simultaneous selection of the optimal feasible prestress can be cast in the following form:

$$\begin{aligned} &\min_{\underline{\underline{\lambda}},G} \quad \mathrm{Tr}[(G^{\mathrm{T}}RG+Q)X] \\ &\text{s.t.} \quad (A(\underline{\underline{\lambda}})+BG)X+X(A(\underline{\underline{\lambda}})+BG)^{\mathrm{T}}+B_wWB_w^{\mathrm{T}}=0, \quad X\succ 0, \quad \underline{\underline{\lambda}}\geqslant 0, \\ &\qquad \lambda_i \leqslant \epsilon\frac{a_iy_i}{l_i}, \ \text{where } \boldsymbol{\lambda}=\Lambda^E\underline{\underline{\lambda}}. \end{aligned} \tag{50}$$

We assume that only bar elements are used for controlling a structure resulting in the following reduction of the number of control variables in (44):

$$\Delta\boldsymbol{\lambda}=\begin{bmatrix}0_{n_{\mathrm{s}}\times n_{\mathrm{b}}}\\ I_{n_{\mathrm{b}}}\end{bmatrix}\Delta\boldsymbol{\lambda}_{\mathrm{b}}. \tag{51}$$

This and the fact that the bars can sustain both compression and tension eliminate the need for imposing additional saturation constraints on the control variables $\Delta\boldsymbol{\lambda}_b$.

### 4.2. An algorithm for designing the structure for optimal LQR performance

The following algorithm provides a monotonic decrease of the cost function of the problem (50) if an initial guess for $\underline{\underline{\lambda}}$ yields a stable matrix $A(\underline{\underline{\lambda}})$.

Step 1. Pick feasible $\underline{\underline{\lambda}}$, $A(\underline{\underline{\lambda}})$.
Step 2. Solve the LQR problem for $X$ and $G$ ignoring the constraint on feasible $\underline{\underline{\lambda}}$.
Step 3. Compute the gradient **grad** of $(G^{\mathrm{T}}RG+Q)X$ with respect to $\underline{\underline{\lambda}}$.
Step 4. Compute the projected gradient **gradproj** with respect to constraint on $\underline{\underline{\lambda}}$.
Step 5. Update $\underline{\underline{\lambda}}$ and $A(\underline{\underline{\lambda}})$ using the line search parameter $\alpha$ that yields a sufficient decrease of the objective, and satisfies that $\underline{\underline{\lambda}}-\alpha$ **gradproj** remains feasible.
Step 6. Repeat Steps 2–5 until optimality conditions are satisfied.

#### 4.2.1. Computing the gradient of the problem objective function

A well-known result from the constrained optimization theory is used for the gradient computation. Consult Fiacco (1983) for more details related to the following lemma.

**Lemma 1.** *The sensitivity* $\partial f(x^*(y))/\partial y$ *of the following optimization problem*:

$$\begin{aligned} &x^*(y)=\arg\min_x \ f(x) \\ &\text{s.t. } c(x,y)=0 \end{aligned}$$

*is*

$$\frac{\partial f(x^*(y))}{\partial y}=\frac{\partial L}{\partial y}\bigg|_{x=x^*,t=t^*}=t^{*\mathrm{T}}\frac{\partial c(x,y)}{\partial y}\bigg|_{x=x^*}, \tag{52}$$

*where* $t^{*\mathrm{T}}$ *is the vector of Lagrange multipliers at the optimal point* $x^*$.

**Proof.** Lagrangian of the problem, defied as

$$L(x,y,t) = f(x) + t^{\mathrm{T}} c(x,y)$$

must satisfy the condition that

$$L(x^*(y), y, t^*(y)) = f(x^*(y)) + t^{*\mathrm{T}}(y) c(x^*(y), y) = f(x^*(y)),$$

at any optimal point $x^*$, $t^*$. Differentiating the Lagrangian at the optimal point, $x^*$, $t^*$, yields

$$\frac{\partial f(x^*(y))}{\partial y} = \frac{\partial L(x^*(y), y, t^*(y))}{\partial y} = \left.\frac{\partial L}{\partial x}\right|_{x=x^*, t=t^*} \frac{\partial x^*(y)}{\partial y} + \left.\frac{\partial L}{\partial t}\right|_{x=x^*, t=t^*} \frac{\partial t^*(y)}{\partial y} + \left.\frac{\partial L}{\partial y}\right|_{x=x^*, t=t^*},$$

which, using the first order optimality conditions: $\left.\frac{\partial L}{\partial x}\right|_{x=x^*, t=t^*} = 0$ and $\left.\frac{\partial L}{\partial t}\right|_{x=x^*, t=t^*} = 0$, gives

$$\frac{\partial f(x^*(y))}{\partial y} = \left.\frac{\partial L}{\partial y}\right|_{x=x^*, t=t^*} = t^{*\mathrm{T}} \left.\frac{\partial c(x,y)}{\partial y}\right|_{x=x^*}. \qquad \square$$

Lemma 1 suggests a method for computing the gradient of the objective function. From the equation in (52), computation of the gradient involves the dual variables $t^*$. The dual problem associated with the Step 2. of the solution algorithm is

$$\begin{aligned} &\min_{\underline{\underline{\lambda}}, G} \ \mathrm{Tr}[B_w W B_w^{\mathrm{T}} T] \\ &\text{s.t.} \quad (A(\underline{\underline{\lambda}}) + BG)^{\mathrm{T}} T + T(A(\underline{\underline{\lambda}}) + BG) + G^{\mathrm{T}} R G + Q = 0, \quad T \succ 0, \end{aligned}$$

so that, after finishing the execution of the Step 2, the dual variables $T = T^{\mathrm{T}} \succ 0$ can be recovered by solving the Lyapunov equation,

$$(A(\underline{\underline{\lambda}}) + BG)^{\mathrm{T}} T + T(A(\underline{\underline{\lambda}}) + BG) + G^{\mathrm{T}} R G + Q = 0.$$

An equivalent form of the Lemma 1 for the problems involving matrices results in the following:

$$\frac{\partial f(G^*(\underline{\underline{\lambda}}))}{\partial \underline{\underline{\lambda}}} = \frac{\partial L^*}{\partial \underline{\underline{\lambda}}},$$

where

$$L^* = \mathrm{Tr}[(G^{\mathrm{T}} R G + Q) X] + \mathrm{Tr}[T((A(\underline{\underline{\lambda}}) + BG) X + X(A(\underline{\underline{\lambda}}) + BG)^{\mathrm{T}} + B_w W B_w^{\mathrm{T}})].$$

Grouping the terms that depend on $\underline{\underline{\lambda}}$, and using the fact that $\mathrm{Tr}[AB] = \mathrm{Tr}[BA] = \mathrm{Tr}[B^{\mathrm{T}} A^{\mathrm{T}}]$ for compatible matrices yields

$$\frac{\partial L^*}{\partial \underline{\underline{\lambda}}} = \frac{\partial}{\partial \underline{\underline{\lambda}}} \mathrm{Tr}[2TA(\underline{\underline{\lambda}}) X] = 2 \frac{\partial}{\partial \underline{\underline{\lambda}}} \mathrm{Tr}[XTA(\underline{\underline{\lambda}})].$$

From (44), it is clear that $\underline{\underline{\lambda}}$ appears only in the $[A(\underline{\underline{\lambda}})]_{2,1}$ block of the matrix $A(\underline{\underline{\lambda}})$, so that

$$\frac{\partial L^*}{\partial \underline{\underline{\lambda}}} = 2 \frac{\partial}{\partial \underline{\underline{\lambda}}} \mathrm{Tr}[[XT]_{1,2} [A(\underline{\underline{\lambda}})]_{2,1}] = 2 \frac{\partial}{\partial \underline{\underline{\lambda}}} \mathrm{Tr}[[XT]_{1,2} \underline{\underline{\mathscr{M}}}^{-1} V_2^{\mathrm{T}} \mathbf{C} \hat{\boldsymbol{\lambda}} \mathbf{M} V_2] = 2 \frac{\partial}{\partial \underline{\underline{\lambda}}} \mathrm{Tr}[\mathbf{M} V_2 [XT]_{1,2} \underline{\underline{\mathscr{M}}}^{-1} V_2^{\mathrm{T}} \mathbf{C} \hat{\boldsymbol{\lambda}}].$$

If the $i$th of $n_{pm}$ columns of the prestress basis $\Lambda^{\mathrm{E}}$ is denoted $\Lambda_i^E$, then,

$$\frac{\partial L^*}{\partial \underline{\underline{\lambda}}} = 2 \frac{\partial}{\partial \underline{\underline{\lambda}}} \mathrm{Tr}\left[\mathbf{M} V_2 [XT]_{1,2} \underline{\underline{\mathscr{M}}}^{-1} V_2^{\mathrm{T}} \mathbf{C} \sum \hat{\Lambda}_i^E \underline{\underline{\lambda}}_i\right] = 2 \frac{\partial}{\partial \underline{\underline{\lambda}}} \sum \underline{\underline{\lambda}}_i \mathrm{Tr}[\mathbf{M} V_2 [XT]_{1,2} \underline{\underline{\mathscr{M}}}^{-1} V_2^{\mathrm{T}} \mathbf{C} \hat{\Lambda}_i^E].$$

Finally, the gradient of the objective function can be written as

$$\mathbf{grad} = \frac{\partial L^*}{\partial \underline{\underline{\boldsymbol{\lambda}}}} = 2 \begin{bmatrix} \mathrm{Tr}[\mathbf{M} V_2 [XT]_{1,2} \underline{\underline{\mathscr{M}}}^{-1} V_2^{\mathrm{T}} \mathbf{C} \hat{\Lambda}_1^E] \\ \mathrm{Tr}[\mathbf{M} V_2 [XT]_{1,2} \underline{\underline{\mathscr{M}}}^{-1} V_2^{\mathrm{T}} \mathbf{C} \hat{\Lambda}_2^E] \\ \vdots \\ \mathrm{Tr}[\mathbf{M} V_2 [XT]_{1,2} \underline{\underline{\mathscr{M}}}^{-1} V_2^{\mathrm{T}} \mathbf{C} \hat{\Lambda}_{n_{pm}}^E] \end{bmatrix}. \tag{53}$$

### 4.3. Example

The planar tensegrity structure depicted in Fig. 3 is optimized. The structure is supported at the two leftmost nodes yielding a stable structure for any feasible choice of the prestress variables $\underline{\underline{\boldsymbol{\lambda}}}$. A vertical

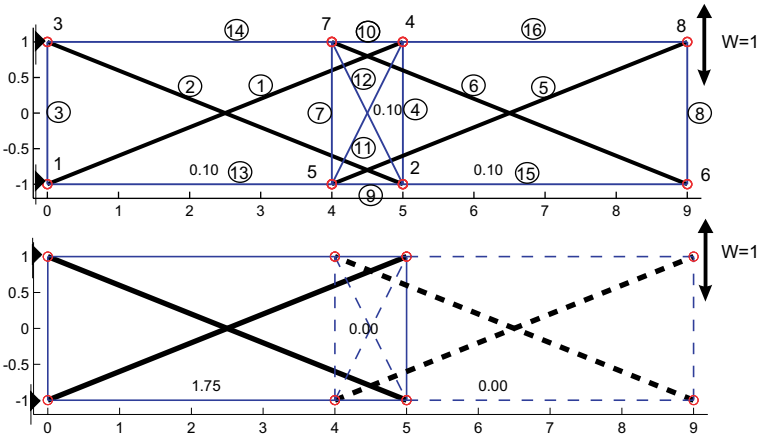


Fig. 3. Initial (up) vs. optimal (down) distribution of the prestress in the tensegrity structure. Dotted lines are used for elements that are not prestressed.

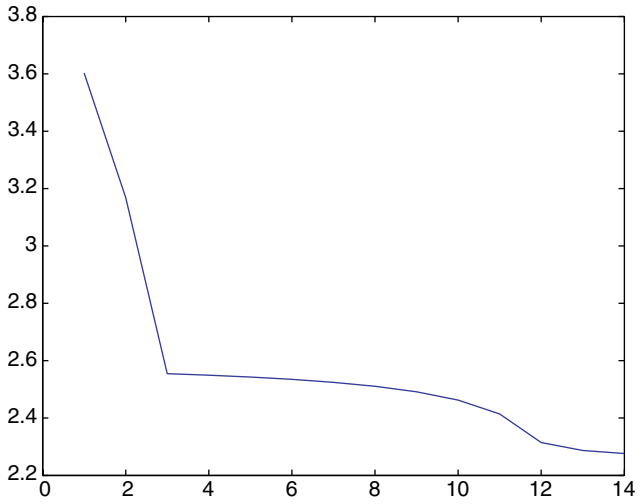

Fig. 4. Convergence of the algorithm-objective vs. iteration number.

zero-mean white noise disturbance of a unit variance acts at the top rightmost node. The initial distribution of the prestress is uniform, $\underline{\underline{\lambda}}^{\mathrm{T}} = [0.1 \;\; 0.1 \;\; 0.1]^{\mathrm{T}}$, as depicted in the upper structure of Fig. 3. The output of interest is the vertical displacement of the top rightmost node, so that, $Q = \mathrm{diag}\{0,\ldots,1,\ldots,0\}$, and we select the control penalty matrix $R = I$. The element and node numbering schemes are shown in Fig. 3, as well as the nodal position vector **p**. The values of the remaining parameters of the problem are, Fig. 4

$$y_i a_i = 10, \quad \mu_i = 0.01, \quad \epsilon_i = 0.5, \qquad i = 1,\ldots,16,$$

$$\mathbf{m} = \begin{bmatrix} 2.6926 \\ 2.6926 \\ 1.0000 \\ 1.0000 \\ 2.6926 \\ 2.6926 \\ 1.0000 \\ 1.0000 \\ 0.5000 \\ 0.5000 \\ 1.1180 \\ 1.1180 \\ 2.0000 \\ 2.0000 \\ 2.0000 \\ 2.0000 \end{bmatrix}, \quad \Lambda^E = \begin{bmatrix} 0.0000 & 0.5292 & 1.1577 \\ 0.0000 & 0.5292 & 1.1577 \\ 0.0000 & 0.5292 & 1.1577 \\ 0.0000 & 0.5292 & 0.0000 \\ 0.5292 & 0.0000 & 1.1577 \\ 0.5292 & 0.0000 & 1.1577 \\ 0.5292 & 0.0000 & 0.0000 \\ 0.5292 & 0.0000 & 1.1577 \\ 2.6462 & 2.6462 & 10.4195 \\ 2.6462 & 2.6462 & 10.4195 \\ 0.0000 & 0.0000 & 1.1577 \\ 0.0000 & 0.0000 & 1.1577 \\ 0.0000 & 0.6615 & 1.4472 \\ 0.0000 & 0.6615 & 1.4472 \\ 0.6615 & 0.0000 & 1.4472 \\ 0.6615 & 0.0000 & 1.4472 \end{bmatrix}.$$

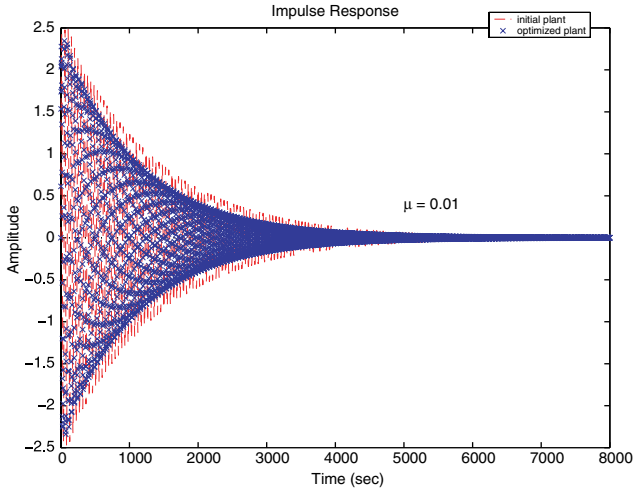


Fig. 5. Impulse response of the initial plant vs. impulse response of the optimized plant—effect of the structure optimization on its dynamic performance.

The optimal distribution of the prestress is not uniform, $\underline{\underline{\lambda}}^{\mathrm{T}} = [0 \;\; 1.7544 \;\; 0]^{\mathrm{T}}$, and it is shown in the lower structure of Fig. 3. The optimal prestress of the two bars closer to the supports is on its upper bound, while the remaining two bars are not prestressed. The effect of the optimal prestress on the open-loop plant is depicted in Fig. 5. This figure shows the vertical displacement of the top right node under a vertical impulsive disturbance of unit intensity acting at the same node. It is obvious that the optimal distribution of the prestress stiffens the plant. The closed-loop behavior of the system is shown in Fig. 6 depicting vertical displacement of the top right node. It is clear that the $L_2$ norm of the plant output is reduced compared to the initial plant for this particular choice of the penalty matrices $R$ and $Q$. The same holds true for the control energy, although these are not general rules independent from the choice of the matrices $Q$ and $R$. Fig. 7 shows the control action of the controlled bar that is attached to the top right node. Clearly, the optimal

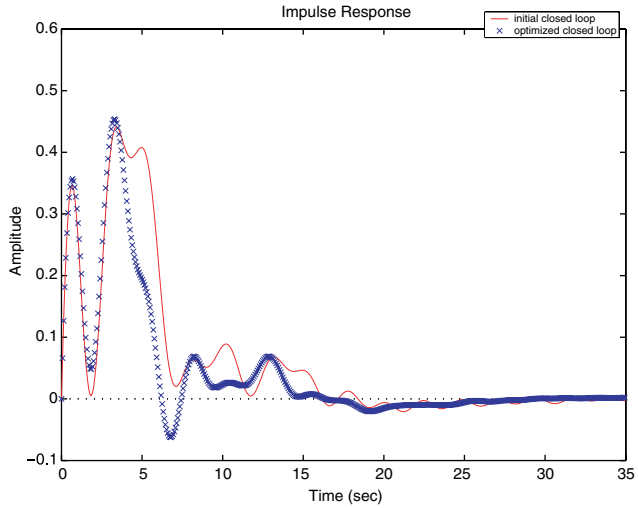


Fig. 6. Closed-loop impulse response of the initial plant vs. the same response for the optimized plant.

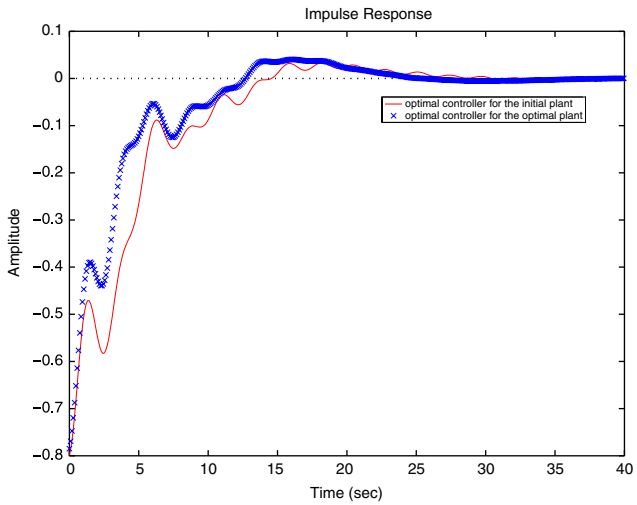


Fig. 7. Output of the controller for the initial and the optimized plant.

LQR controller for the optimized plant requires less control energy than the initial optimal controller for the suboptimal plant.

Our studies have shown that the optimal distribution of prestress is not independent from the formulation of the objective function. For example, penalizing positions of all free nodes using $Q = \text{blockdiag}\{I, 0\}$ yields the following optimal prestress, $\underline{\underline{\lambda}}^{\mathrm{T}} = [1.7544 \;\; 1.754 \;\; 0]^{\mathrm{T}}$, for the same set of input parameters. The optimal prestress of all bars is on its upper bound in this case.

## 5. Conclusions

Structure and control designs have traditionally been two separate processes that can yield significant performance limitations when performed independently. This paper addresses specifics of integrated plant and control design of tensegrity structures and demonstrates a method for their prestress optimization. A gradient based algorithm is proposed for solving the prestress selection problem. Because of the non-convex nature of the problem, there is no guarantee that a solution is a global optimum. Nonetheless, this algorithm guaranties a monotonic improvement of the performance index, and therefore can be considered as a legitimate design tool.

The presented derivation of the dynamic model of tensegrity structures (trusses) is performed using global coordinates of an assembled structure, and it results in a compact model with a clearly displayed algebraic structure. This derivation bypasses modelling dynamics of elements in local coordinates and does not require transformations to global coordinates, and the subsequent assembly, which all together may obscure the algebraic structure of the model. This is particularly important for studies that involve rank analysis of related matrices, and computations of performance gradients similar to those presented in this paper. One of the novelties introduced by this paper is a demonstration of the decomposition of the structure prestress into the extreme directions of the prestress cone.

## References

Adeli, H., Saleh, A., 1998. Integrated structural/control optimization of large adaptive/smart structures. International Journal of Solids and Structures 35 (28–29), 3815–3830.

Alkire, B.F., 2003. Convex optimization problems involving autocorrelation sequences. PhD thesis, University of California, Los Angeles.

Boyd, S., Ghaoui, E.L., Feron, E., Balakrishnan, V., 1994. Linear matrix inequalities in system and control theoryStudies in Applied Mathematics, vol. 15. Society for Industrial and Applied Mathematics (SIAM).

Camino, J.F., Maurício Carvalho de Oliveira, Skelton, R.E., 2002. Plant and control design using convexifying LMI methods. In: Proceedings of the 15th IFAC Conference, 2002, Barcelona, Spain, pp. 2405–2410.

Camino, J.F., Maurício Carvalho de Oliveira, Skelton, R.E., 2003. 'Convexifying' linear matrix inequality methods for integrating structure and control design. Journal of Structural Engineering-ASCE 129 (7), 978–988.

Connelly, R., Whiteley, W., 1996. Second order rigidity and prestress stability for tensegrity frameworks. SIAM Journal of Discrete Mathematics 9 (3), 453–491.

Fiacco, A.V., 1983. Introduction to Sensitivity and Stability Analysis in Nonlinear Programming. Academic Press, New York.

Hughes, T.J.R., 1987. The Finite Element Method: Linear Static and Dynamic Finite Element Analysis. Prentice Hall.

Kanchanasaratool, N., Williamson, D., 2002. Modeling and control of class nsp tensegrity structures. International Journal of Control 75 (2), 123–139.

Khot, N.S., 1998. Multicriteria optimization for design of structures with active control. Journal of Aerospace Engineering-ASCE 11 (2), 45–51.

Kwakernaak, H., Sivan, R., 1972. Linear Optimal Control Systems. Wiley.

Lu, J.B., Skelton, R.E., 2000. Integrating structure and control design to achieve mixed h-2/h-infinity performance. International Journal of Control 73 (16), 1449–1462.

Masic, M., Skelton, R.E., 2004. Optimization of class-2 tensegrity towers. In: Proceedings of the 11th Smart Structures and Materials Conference, vol. 5390, International Society for Optical Engineering (SPIE), Bellingham, WA, USA, pp. 163–174.

Masic, M., Skelton, R.E., 2005. Path planning and open-loop shape control of modular tensegrity structures. AIAA Journal of Guidance, Control, and Dynamics 28 (3), 421–430.

Masic, M., Skelton, R.E., Gill, P.E., 2005a. Algebraic tensegrity form-finding. International Journal of Solids and Structures 42 (16–17), 4833–4858. doi:10.1016/j.ijsolstr.2005.01.014.

Masic, M., Skelton, R.E., Gill, P.E., 2005b. Optimization of tensegrity structures. p. in review.

Micheletti, A., 2003. The indeterminancy conditions for tensegrity towers. Revue Francais de Genie Civil 7 (3), 329–342.

Murakami, H., 2001. Static and dynamic analysis of tensegrity structures. Part 1. Nonlinear equations of motion. International Journal of Solids and Structures 38 (20), 3599–3613.

Pellegrino, S., 1992. A class of tensegrity domes. International Journal of Space Structures 7 (2), 127–142.

Saleh, A., Adeli, H., 1994. Parallel algorithms for integrated structural/control optimization. Journal of Aerospace Engineering, ASCE 7 (3), 297–314.

Skelton, R.E., 1988. Dynamic Systems Control—Linear Systems Analysis and Synthesis. John Wiley & Sons.

Skelton, R.E., 1995. Integrated plant and controller design. American Control Conference, Seattle, June 21–23.

Skelton, R.E., Hanks, B.R., Smith, M., 1992. Structure redesign for improved dynamic-response. Journal of Guidance, Control and Dynamics 15 (5), 1272–1278.

Skelton, R.E., Pinaud, J.P., Mingori, D.L., 2001. Dynamics of the shell-class of tensegrity structures. Journal of the Franklin Institute 2–3 (338), 255–320.

Sultan, C., Corless, M., Skelton, R.E., 2002. Symmetric reconfiguration of tensegrity structures. International Journal of Solids and Structures 39 (8), 2215–2234.

Tibert, A.G., Pellegrino, S., 2003. Review of form-finding methods for tensegrity structures. International Journal of Space Structures.

Vasart, N., Motro, R., 1999. Multiparametered form finding method: application to tensegrity systems. International Journal of Space Structures 14 (2), 147–154.

Williamson, D., Skelton, R.E., Han, J., 2003. Equilibrium conditions of a tensegrity structure. International Journal of Solids and Structures 40, 6347–6367.

Zhou, K., Doyle, J.C., 1998. Essentials of Robust Control. Prentice Hall, Upper Saddle River, NJ 07458 (Chapter 13, pp. 255–261).